

# Calculation of Separated Boundary-Layer Flows

Tuncer Cebeci\*

*California State University at Long Beach, Long Beach, Calif.*

E.E. Khalil†

*University of Cairo, Cairo, Egypt*

and

J.H. Whitelaw‡

*Imperial College, London, England*

## Abstract

THE local velocity characteristics of separating boundary-layer flows and the resulting downstream regions of recirculation are obtained by solving, with finite-difference methods, parabolic and elliptic equations that represent conservation of mass and momentum. Both methods are shown to represent, in general terms, the measurements of Simpson et al.<sup>1</sup> obtained in a separating boundary layer. Quantitative discrepancies exist and may be attributed partly to the turbulence models and wall functions. In addition, the boundary-layer assumptions of the parabolic equations may contribute to the discrepancies, and the comparatively small number of nodes available for the solution of the elliptic equations undoubtedly contribute. The elliptic procedure has been used to calculate the separated flow in wide-angle diffusers and on wedges, again with flow separation, intended to simulate the trailing edge of airfoils at angle of attack.

## Contents

The investigation is aimed at the development of a method for the calculation of the flow characteristics in the vicinity of an airfoil at high angle of attack. The paper demonstrates that related calculations can be performed with either elliptic equations or with a combination of potential flow and boundary-layer equations. The former are, in principle, more appropriate but, in practice and for small regions of recirculation, are less economical and precise. In the longer term, it is desirable to quantify the precision of both methods as a function of angle of attack. Results have been obtained with both sets of equations, for boundary conditions corresponding to the separating boundary-layer flows of Simpson, Strickland, and Barr.<sup>1</sup> Although the comparison of the two methods is inexact in many respects (for example, different turbulence models are used in the two solution procedures, and different boundary-condition specifications may influence the results), it allows a preliminary assessment of several aspects of their use.

The steady two-dimensional form of the Navier-Stokes equations was solved with a numerical procedure based on the TEACH code of Gosman and Pun.<sup>2</sup> Converged solutions were accepted when all normalized residuals were less than

$10^{-3}$ . The resulting computer times were of the order of 400 s on a CDC 6600. The boundary-layer equations, using the Cebeci-Smith eddy viscosity formulation, were solved with the numerical scheme used extensively by Keller and Cebeci and described in detail in Ref. 3. It was used with prescribed freestream velocity until separation was imminent when the inverse method described in Ref. 3 was used. With the elliptic procedure, the turbulence was characterized by further elliptic equations representing conservation of turbulent kinetic energy and dissipation rate.

Where possible, known values were specified as boundary conditions. Initial profiles of kinetic energy and its dissipation rate were estimated on the basis of mixing length assumptions. The downstream boundary condition for the elliptic procedure was assumed to be  $\partial\phi/\partial x = 0$  at a location where the assumption did not influence upstream results. The parabolic procedure made use of the measured displacement-thickness distribution downstream of separation, whereas the entire flow was considered with the elliptic equations. In both cases, the node points adjacent to walls were linked to the wall by logarithmic wall functions.

A nonuniform, rectangular, finite-difference mesh was used with the elliptic equations and encompassed the wind tunnel. The crossflow nodes were assigned with 20 nodes at the exit from the test section and 12 nodes within the experimentally determined boundary-layer thickness at  $x = 4.46$  m (175.7 in.). The rectangular mesh implied 11 nodes across the test section at its narrowest point and 15 at the entrance. The near-wall nodes were located at a distance of 2.5 mm (0.1 in.) from the wall. A uniform velocity was assigned at the entrance to the test section together with zero cross-stream velocity, uniform turbulence energy corresponding to an intensity of 0.1%, and uniform dissipation rate given by  $\epsilon = k^{3/2}/(0.005 \times \text{duct width})$ . At the exit from the test section, all  $x$  gradients were assumed zero, and 5.5% of the total mass was allowed to escape, in accordance with experiment, at the node located closest to the roof of the tunnel, and at  $x$  values between 20.304 and 2.638 m (90.7 and 103.8 in.). The existence of the corresponding normal velocity between the two nodes of the staggered grid was essential to the calculation of separation, but the locations of the two nodes, provided the normal velocity corresponded to the experimental mass flows, had a much smaller influence.

Figure 1 presents calculated velocity profiles and shows a region of flow separation similar to that measured by Simpson et al. Quantitative differences exist and are probably greater than can be attributed to experimental uncertainty. The freestream velocity distribution, based on maximum values at each cross-stream location, was also obtained and suggested a milder pressure distribution than that measured; the gradient in the vicinity of separation was, however, similar. The integral thicknesses were computed with linear interpolation between nodes and the distributions of  $R_\theta$  and  $H$  are in remarkably good agreement with measurement. The

Presented as Paper 79-0284 at the AIAA 17th Aerospace Sciences Meeting, New Orleans, La., Jan. 15-17, 1979; submitted Jan. 29, 1979; synoptic received Feb. 20, 1979; revision received June 11, 1979. Full paper available from AIAA Library, 555 West 57th Street, New York, N.Y. 10019. Price: Microfiche, \$2.00; hard copy, \$5.00. **Order must be accompanied by remittance.** Copyright © 1979 by Tuncer Cebeci. Published by the American Institute of Aeronautics and Astronautics with permission.

Index categories: Boundary Layers and Convective Heat Transfer – Turbulent; Computational Methods.

\*Distinguished Professor. Member AIAA.

†Lecturer.

‡Professor.

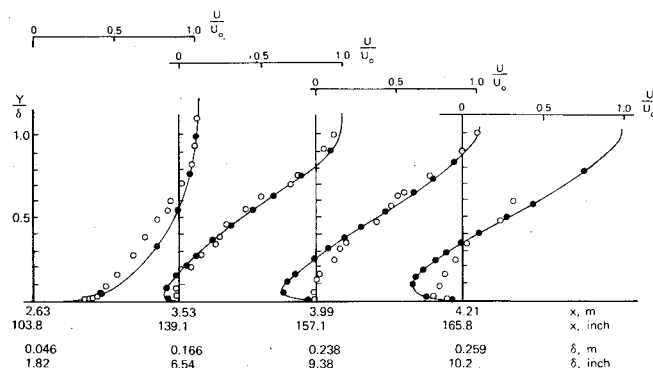


Fig. 1 Comparison of measured and calculated mean velocity profiles (○: LDV results of Ref. 1; ●: elliptic calculations).

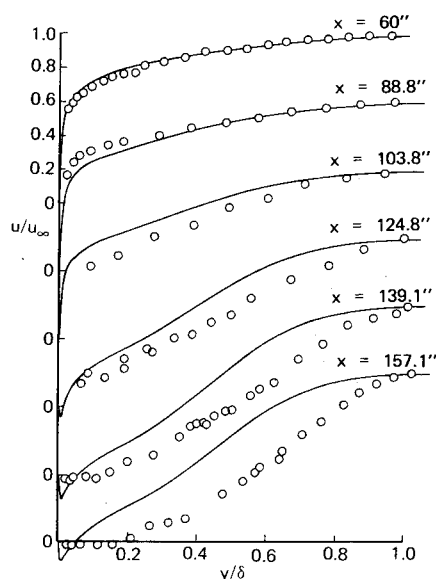


Fig. 2 Comparison of mean velocity profiles normalized with experimental values of  $U_\infty$  (○: LDV results of Ref. 1; —: inverse boundary-layer calculations).

agreement between measured and calculated values of skin-friction coefficient were less satisfactory.

The boundary-layer calculations were begun with the velocity profile measured at 1.524 m (60 in.) and assumed the measured distribution of freestream velocity. No region of reverse flow was detected and the calculation proceeded to the end of the base plate, with 50 nodes in each cross-stream plane, in 10 s. The calculation was repeated, this time with a freestream boundary condition corresponding to the measured distribution of displacement thickness. This inverse procedure did encounter a region of separated flow and allowed the determination of a freestream velocity distribution which corresponded to a stronger pressure gradient than that measured. The results, shown in Fig. 2, demonstrate reasonable agreement with experiment in the attached region of flow.

The elliptic equations are more complete, but the finite number of nodes implies that the solutions to the finite-difference equations are only approximate solutions to the differential equations. Only 286 nodes were located in the flowfield and, although it is the comparatively uninfluential upstream region which is least represented, errors larger than 5% can be expected. On the other hand, the boundary-layer equations, although less complete, are solved by a more

precise numerical scheme with many more effective nodes. An indication of the magnitude of the terms considered by the elliptic equations and rejected by the parabolic equations may be obtained from the present solutions. The number of nodes located in the region of separated flow is too small to allow firm conclusions, but the results clearly show cross-stream pressure gradients of the same order of magnitude as the longitudinal pressure gradient.

The preceding results must be viewed with considerable caution but, nevertheless, demonstrate that separated boundary-layer flows can reasonably be represented by numerical solutions of appropriate conservation equations in differential form.

The numerical procedure used to solve the boundary-layer equations has been used extensively in the past and can be expected not to introduce significant errors. Thus the differences indicated by Fig. 2 and the calculated and measured "freestream velocity" distributions may be due, in part, to either of the boundary-layer equations, the eddy-viscosity formulation, the wall functions, or the measurements, and it is impossible to determine which on the basis of the present evidence. The present boundary-layer equations make use of wall-functions which effectively solve into the viscous sublayer and, certainly within the context of the corresponding eddy-viscosity hypothesis, are adequate only for attached flows. The present inverse boundary-layer procedure provides an excellent vehicle with which to examine alternative procedures, including the need to consider the influence of normal stresses as suggested by in Ref. 1.

The use of elliptic equations also presents difficulties in the prescription of the freestream boundary condition and, in the present case, a satisfactory free boundary condition could not be found easily. The application of a solution domain encompassing the entire wind tunnel may be indicative of the need, in future stalled airfoil cases, to apply a freestream condition outside the regions of potential and rotational flow. In the present case, the consideration of the whole wind tunnel limited the number of grid nodes located in the wall boundary layer and associated region of separation and emphasizes the approximate nature of the solution. Separation was, however, calculated and in the correct region of the surface. Clearly, the present coordinate system is inappropriate to the flow configuration considered here and must be improved.

The elliptic procedure was used to calculate the flow in plane, wide-angle diffusers and on wedges. In the former case, comparison with measurements showed that even though flow symmetry was assumed where it did not exist, the pressure coefficient distribution was well represented. The wedge calculations indicate that the procedure can assist the representation of the separated flow on airfoils at high angle of attack and in the downstream wake.

### Acknowledgment

Financial support from the Office of Naval Research (Contract No. N00014-77-C-0077), the Atomic Energy Research Establishment, and the Science Research Council is gratefully acknowledged.

### References

1. Simpson, R.L., Strickland, J.M., and Barr, P.W., "Laser Hot-Film Anemometer Measurements in a Separating Turbulent Boundary Layer," *Journal of Fluid Mechanics*, Vol. 79, 1977, p. 555.
2. Gosman, A.D. and Pun, W.M., "Calculation of Recirculating Flows," Mechanical Engineering Department Rept. HTS/74/2, Imperial College, London, 1974.
3. Cebeci, T. and Bradshaw, P., *Momentum Transfer in Boundary Layers*, McGraw-Hill/Hemisphere Publishing Co., Washington, D.C., 1977.